6494 *Macromolecules* **2002,** *35,* 6494−6504

Articles

Poly(propylene carbonate). 1. More about Poly(propylene carbonate) Formed from the Copolymerization of Propylene Oxide and Carbon Dioxide Employing a Zinc Glutarate Catalyst

Malcolm H. Chisholm,* Diana Navarro-Llobet, and Zhiping Zhou

Department of Chemistry, The Ohio State University, 100 W. 18th Avenue, Columbus, Ohio 43210

Received March 6, 2002; Revised Manuscript Received May 24, 2002

ABSTRACT: Propylene oxide, PO, reacts when heated to 60 °C over a zinc glutarate catalyst to form poly(propylene oxide), PPO, which is regioregular, HTHTHT, and favors isotactic triads **ii**. Under 50 bar of CO_2, poly(propylene carbonate), PPC, is formed with less than 5% polyether linkages and with an even smaller component of propylene carbonate, PC. These reactions have been studied as a function of time, and the products have been analyzed by GPC, MALDI−TOF/MS, and $^{13}C\ \{^1H\}$ NMR spectroscopy. Polymerization of PO yields PPO with −OH and −H end groups, and in the copolymerization of PO and CO_2 the low molecular weight chains are readily identified as an alternating copolymer represented as $(PO)_n$-*alt*-$(CO_2)_m$, where $m = n - 1$, $n - 2$, $n - 3$, $n - 4$, $n - 5$, with terminal −OH and −H groups. These results, combined with NMR data, implicate Zn−OH groups as the active initiating species, and furthermore from the molecular weight of the polymer produced at short reaction times, we can infer that some Zn−OH sites are highly active in producing long-chain polymers. The $^{13}C\ \{^1H\}$ NMR spectra of PPC formed from *rac*-PO, 50:50 *S*-PO + *rac*-PO, and *S*-PO reveal the preferential formation of HT junctions in the ring-opening of PO by the alkyl carbonate with a HH:HT:TT ratio of 1:3:1. Certain assignments at the diad, triad, and tetrad levels are offered.

Introduction

Since the discovery in 1969 that a heterogeneous catalyst system employing $ZnEt_2/H_2O$, propylene oxide, PO, and carbon dioxide gave a polymer involving the regular alternating copolymer poly(propylene carbonate), PPC,[1] there has been a long-standing interest in this process.[2] Several heterogeneous catalyst systems are known to effect this polymerization,[3] along with a homogeneous system derived from $ZnEt_2$/pyrogallol and an aluminum porphyrin system described by Kuran[4] and Inoue,[5] respectively. The polymer PPC has many attractive features. It is formed from inexpensive and readily renewable sources, and its physical properties would allow it to be readily processed as films with a potential utility as a biodegradable packaging material. Despite these attractive features, commercialization has never been achieved because no catalyst system is sufficiently efficient. For example, zinc glutarate, in neat PO/CO_2, is reported to be the most active system, yet 1 g of catalyst produces only 70 g of PPC in 40 h.[6] This poses a challenge to the chemist to find a more catalytically active system. Moreover, well-defined single site catalysts such as (BDI)Zn(OR), (R = ^{i}Pr),[7] shown in **A**, appear ineffective in forming the copolymer PPC but are active in the formation of propylene carbonate, PC.[8]

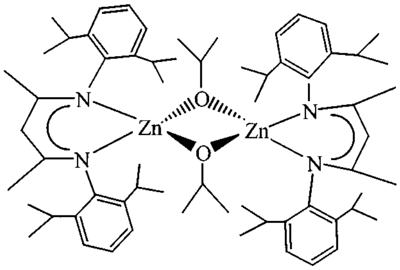

A

The reactions leading to PC and PPC are clearly competing, but it is not obvious why the formation of PPC should be favored in some instances. Simple base catalysis favors the formation of the five-membered ring product PC as in the reaction between PO and CO_2 that is catalyzed by alkylammonium or phosphonium halides.[9]

Prompted by these considerations, we have taken up the challenge of catalyst design for PPC formation. We report here our studies of the zinc glutarate production of PPC.

Results and Discussion

1. $^{13}C\ \{^1H\}$ NMR Spectra of PPC. Only one previous literature report has dealt with the microstructure of PPC, and the focus of that work was on the carbonate carbon.[10] Three regions in the $^{13}C\ \{^1H\}$ NMR spectrum of the carbonate carbon were assigned as HT, TT, and HH as shown in Figure 1. These junctions are shown in Scheme 1, and given that the PPC chain was formed

10.1021/ma020348+ CCC: $22.00 © 2002 American Chemical Society
Published on Web 07/10/2002

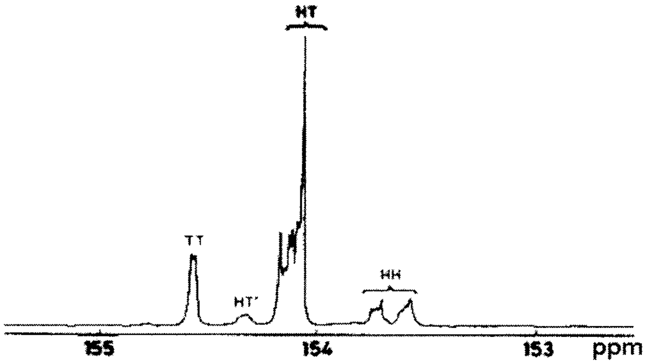

Figure 1. ^{13}C {^{1}H} (100 MHz, $CDCl_3$) NMR spectrum of the C=O region of PPC reported in ref 8 [reproduced with permission].

Scheme 1. Three Possible Regiosequences of PPC at the Diad Level When Looking at the Central Carbonate Carbon

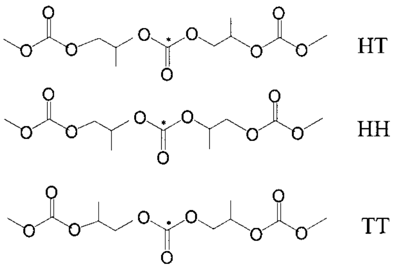

Scheme 2. Ring-Opening of PO by a Back-Side Attack Mechanism

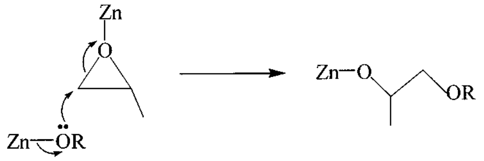

Scheme 3. Eight Possible Regiosequences for Carbonate Carbons (*) in PPC with Central HT Junctions at the Tetrad Level: (4, 5), (2, 6), (3, 7), and (1, 8) Are Four Distinguishable Sequences by NMR Spectroscopy

Diad level	Tetrad level	
(HT).(HT)	(HT)(HT).(HT)(HT)	1
	(HT)(HT).(HT)(TH)	2
	(TH)(HT).(HT)(HT)	3
	(TH)(HT).(HT)(TH)	4
(TH).(TH)	(HT)(TH).(TH)(HT)	5 = 4
	(HT)(TH).(TH)(TH)	6 = 2
	(TH)(TH).(TH)(HT)	7 = 3
	(TH)(TH).(TH)(TH)	8 = 1

from *rac*-PO, each regiosequence can be further broken down to **i** or **s** stereosequences. As is evident from an inspection of Figure 1, there are more than two resonances in the HT and HH regions, and this implies that the carbonate carbon must be sensitive to more than its adjacent PO units.

We have no reason to challenge this original assignment made at the diad level, and we build on this in the studies reported herein. We have examined the PPC prepared from a zinc glutarate catalyst at ^{13}C frequencies of 100, 150, and 200 MHz. Three different samples of PPC were employed, namely those derived from *rac*-PO, 50:50 *rac* + *S*-PO, and 99% *S*-PO, having M_n of 17 000−67 000 Da and PDIs of 7.0−14.0.

The Carbonate Carbon Region. The ^{13}C {^{1}H} NMR spectra of the carbonate carbon signals are shown in Figure 2 for the three different samples. Details pertaining to concentration and spectra acquisition are given in the Experimental Section. The ratio of the TT:HT:HH junctions is on the order 1:3:1. The HT junctions are thus favored over their statistical occurrence, and this indicates that the ring-opening of PO occurs with some regiospecificity in the formation of PPC. This is not altogether surprising inasmuch as the zinc glutarate catalyst ring opens PO (in the absence of CO_2) to give regioregular PPO (HTHTHT) as shown in Figure 3. In the case of PPO formation, we anticipate a transition state for ring-opening involving backside attack on a zinc bound PO molecule by a neighboring alkoxide group which in turn is bound to a zinc(II) center (Scheme 2). In this way the regioregular (HTHTHT) PPO is formed, and in coordinate catalysis this has been seen to favor the formation of isotactic junctions when the PO monomer is racemic.[11] In the case of ring-opening of PO in PPC formation, a carbonate oxygen is the nucleophile. This is less sterically demanding and apparently less discriminating in its attack on a PO carbon. From the observed TT:HT:HH junctions, we can estimate that the relative attack on a tail, T, the CH_2 carbon, vs the head, H, the CH carbon, to be in the ratio of 3:1. See Supporting Information.

The simplest of the spectra shown in Figure 2 arises from the copolymerization of *S*-PO and CO_2. Each region (HH, HT, and TT) shows more than one resonance providing information concerning the possible regiosequences that occur at the tetrad level. As shown in the drawings in Scheme 3, there are four regiosequences with central H−T junctions that are distinguishable by NMR for the carbonate carbons. The relative abundances of these regiosequences can be calculated on the basis of the 3:1 preference for HT over HH or TT junction formation. In this way we can assign the predominant carbonate signal of PPC derived from *S*-PO to the **iii** tetrad of the (HT)(HT).(HT)(HT) sequence, which must, by accidental degeneracy, occur with one of the other less abundant regiosequences (HT)(HT).(HT)(TH) or (TH)(HT).(HT)(HT). The minor signal is assigned to one of the latter and the least favored (TH)(HT).(HT)(TH) sequence. Polymerization of the 50:50 mixture of *S*-PO + *rac*-PO in the formation of PPC will favor the eight stereosequences of the (HT)(HT).(HT)(HT) tetrad as follows: **iii** (0.320), **iis** (0.117), **sii** (0.117), **iss** (0.117), **ssi** (0.117), **isi** (0.070), **sis** (0.070), and **sss** (0.070). See Supporting Information. However, because other regiosequences are in combination roughly equally probable to the major (HT)(HT).(HT)(HT) tetrad, we are unable to make any further unequivocal assignments.

The other carbonate carbon signals arise from TT and HH junctions at the diad level. Again, assuming backside attack, we can assign the TT region as **s** at the diad level and the HH region similarly. Inspection of the HH region clearly shows evidence of several partially overlapping resonances, and we can make tentative assignments at the tetrad level based on knowledge of the preference for TH/HT formation.

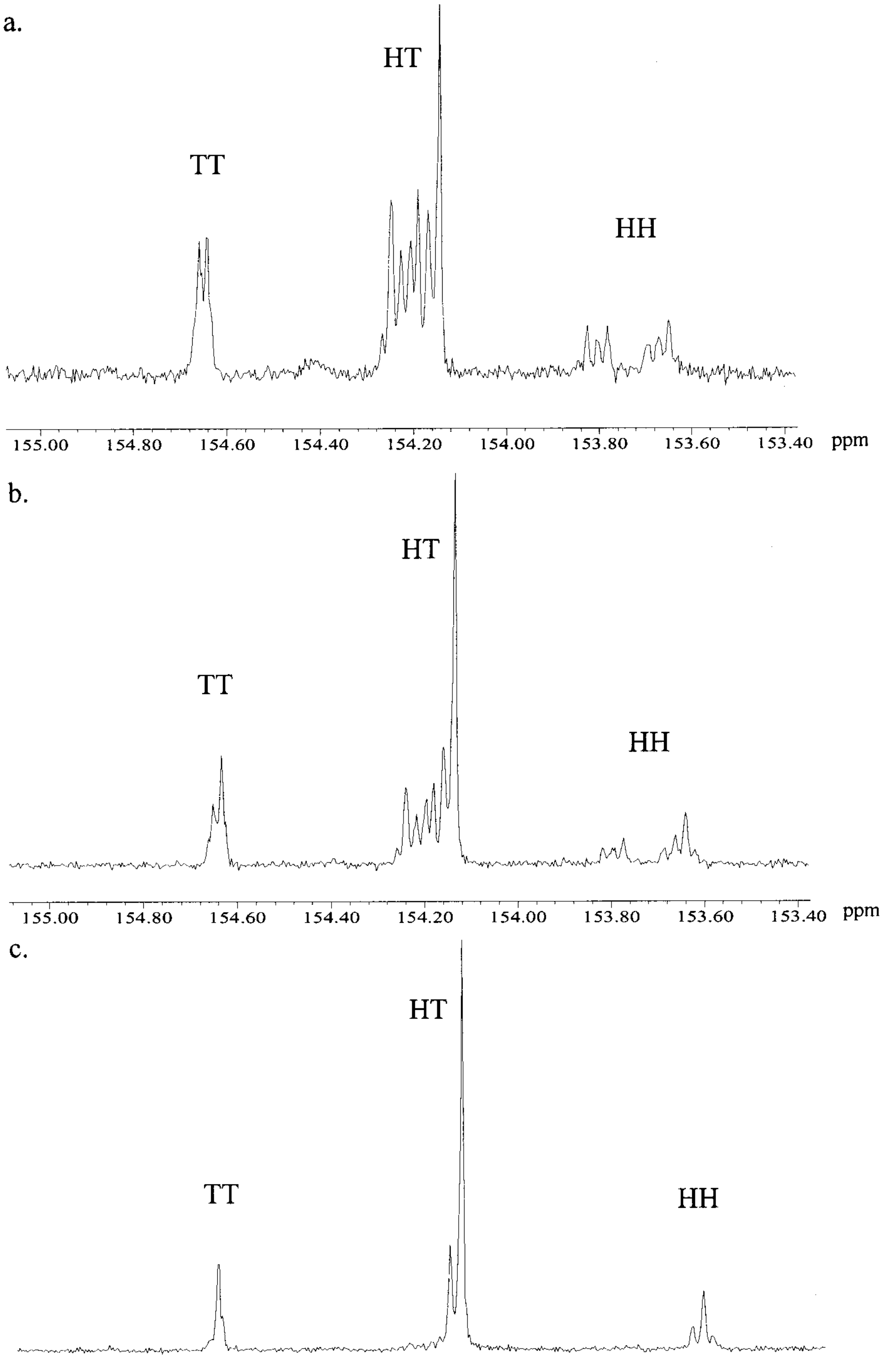

Figure 2. ^{13}C $\{^1H\}$ (150 MHz) NMR spectra of C═O region of PPC made from (a) *rac*-PO, (b) 50% *rac*-PO and 50% *S*-PO, and (c) *S*-PO, employing a zinc glutarate catalyst.

The Methine, Methylene, and Methyl Carbon Regions. The assignments of the carbon signals derived from PO are complementary to those of the carbonate carbon. However, because of the structure of the polymer, their sensitivity is examined at the triad level. There are eight possible regiosequences for CH, CH_2, and CH_3 carbons at the triad level as the polymer is inherently asymmetric. Only four regiosequencies are distinguishable by NMR spectroscopy. These are shown in Schemes 4–6.

The ^{13}C $\{^1H\}$ spectrum derived from *S*-PO reveals four regiosequences as shown in Figure 4. The most abundant signal at δ 72.34 ppm can be assigned to the most abundant regiosequence (HT)(H.T)(HT) (Scheme 4) which, assuming backside attack, must be **ii**. Of the three other signals we notice that two are upfield at ca. δ 72.1 ppm while the other is very close to the signal of the regioregular sequence. All are roughly of the same integral intensity so an unequivocal assignment cannot be made. We are, however, inclined toward the view that the two upfield signals arise from sequences that have TH junctions. See Scheme 4.

In going from *S*-PO to *rac*-PO, the overlap of the resonances is very pronounced. Nevertheless, we feel

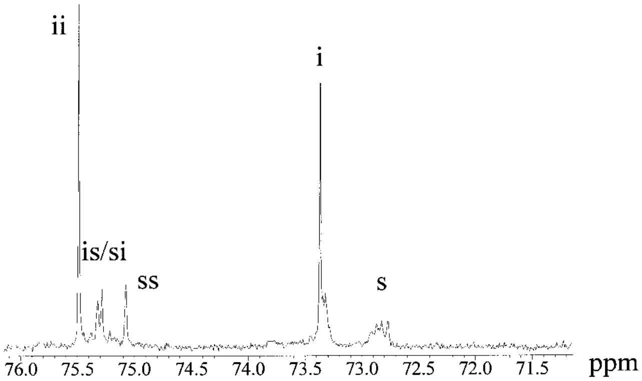

Figure 3. $^{13}C\ \{^1H\}$ (100 MHz) NMR spectrum showing the methine and methylene carbons of PPO prepared with a zinc glutarate catalyst.

Scheme 4. Eight Possible Regiosequences for Methine Carbons (*) in PPC at the Triad Level: (4, 5), (2, 6), (3, 7), and (1, 8) Are Four Distinguishable Sequences by NMR Spectroscopy[a]

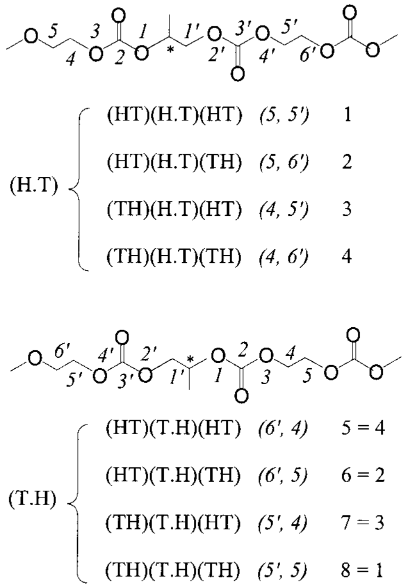

[a] The numbers in the brackets indicate the positions of the neighboring methine groups for that regiosequence.

we can, on the basis of deconvolution, assign the **ii**, **ss**, and **is**/**si** signals of the most abundant triad sequence (HT)(H.T)(HT).

The methylene region of PPC derived from *S*-PO shows just two resonances of integral intensity 37% and 63% (Figure 5). This can only arise from accidental degeneracy of the major (HT)(H.T)(HT) regiosequence signal with one of the minor. On the basis of considerations of bond distances, we propose that the regiosequence with a HH junction is coincident with the regioregular sequence. The upfield methylene resonance is thus assigned to the two regiosequences with TT junctions. On the basis of the statistics of HT ring-opening being favored in the ratio 3:1, as deduced from the carbonate carbon signals, we predict the ratio of 37:63, which fits exactly that observed. Once again in going from polymerizations involving *S*-PO to *rac*-PO, new resonances appear which must correspond to **s** sequences. It is, however, not possible to correlate these reliably with the regiosequences.

The methyl carbon region obtained from PPC prepared with *S*-PO shows only three signals in the integral ratio 17:62:21 in Figure 6. The major signal can once again be assigned to the **ii** triad of the major regiosequence (HT)(H.T)(HT) with a coincidence with one of the minor regioirregular triads. This would have a calculated combined integral intensity of 62.5%. In changing from *S*-PO to *rac*-PO, only the downfield signals increase in intensity. While it is again clear that there is considerable overlap (accidental degeneracy), it would seem that the **is**/**si** and **ss** stereosequences of the regioregular (HT)(H.T)(HT) triad must be embodied within this large and broad upfield signal.

Table 1. Percentage of PPC, PC, and Polyether Linkage Formed in the Copolymerization of *rac*-PO and CO_2 as a Function of Time

reaction time (h)	PPC (%)	PC (%)	polyether linkage[a] (%)	PO monomer[b]
2.5	16.5	0.6	2.23	80.6
5	71.1	2.4	2.22	24.3
5[c]			72.4	27.6
10	68.8	3.8	2.17	25.2
20	77.4	4.4	2.17	16.0
40	90.5	5.7	2.15	1.6

[a] Two or more units of PO linked together. [b] PO Monomer left after the reactions. [c] Homopolymerization of PO in the absence of CO_2.

2. PPC Formation as a Function of Time. As noted in the Introduction, one of the major problems in the production of PPC is that its formation is very slow and inefficient with respect to monomer-to-catalyst ratio; i.e., 70 g of PPC per 1 g of catalyst in 40 h represents the highest reported efficiency.[6] We have examined the formation of PPC in the zinc glutarate-catalyzed reaction as a function of time. With a heterogeneous catalyst we always have to be concerned that the number of active sites will vary with catalyst preparation, i.e., with surface area and impurities. To minimize these effects in our studies, we have used data obtained from one specific catalyst preparation and we have stored the catalyst in a drybox with less than 1 ppm of O_2/H_2O. Each catalyst run employed the same PO to zinc glutarate concentration (2 mL of PO and 100 mg of zinc glutarate catalyst), a CO_2 pressure of 50 bar, and temperature of 60 °C. The reactor was loaded in the drybox, transferred to the benchtop, purged with CO_2, and then pressurized. Each reaction was stirred with the aid of a magnetic follower. The reactions were monitored as a function of time in the following way. At time *t* h, the reactor was cooled to room temperature and the pressure was slowly released. The reaction mixture was then examined by ^1H NMR spectroscopy to determine or gain a reasonable estimate of the percent conversion of PPC along with the other impurities, namely PC and polyether linkages that have the appearance of PPO by ^1H NMR spectroscopy. The data are summarized in Table 1.

A number of points are noteworthy. (1) The percent of PPC conversion with time increases to 90% at 40 h, but after 5−10 h 70% conversion is already achieved. (2) The percent of PC formation increases slowly with time whereas the percent of polyether linkages remains essentially constant. (3) At high percent PPC formation, the reactor contains the product as solid foam. (4) In the absence of CO_2, PO is polymerized to regioregular PPO at a rate comparable to PPC production (in the presence of CO_2) during the initial 5−10 h. The PDI of the PPO is also comparable to that of the PPC, ~7, suggesting many different reactive sites.

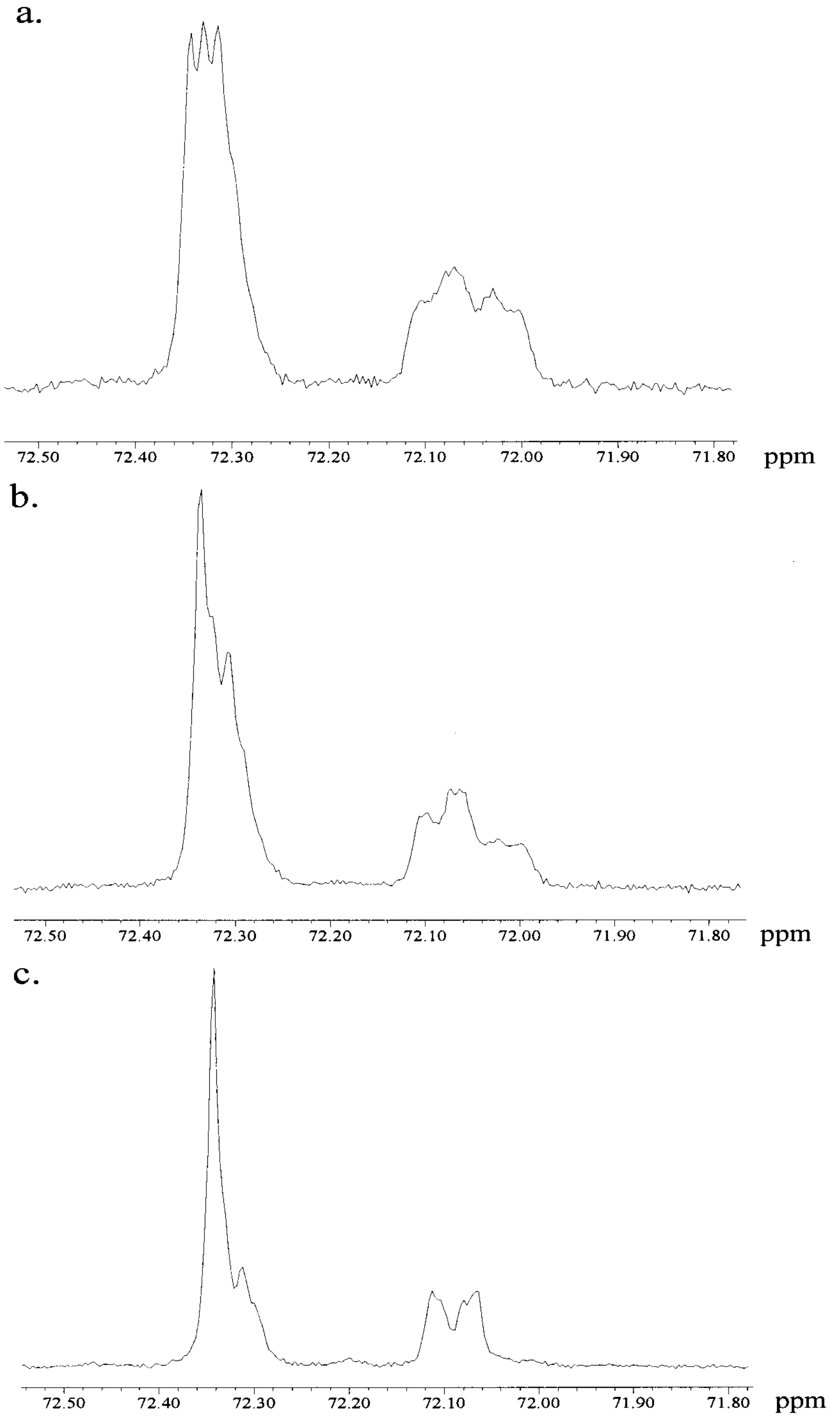

Figure 4. $^{13}C\ \{^{1}H\}$ (150 MHz) NMR spectra of CH region of PPC made from (a) *rac*-PO, (b) 50% *rac*-PO and 50% *S*-PO, and (c) *S*-PO, employing a zinc glutarate catalyst.

We worked up the PPC by dissolving the foam (or viscous solution) in benzene and removing the zinc glutarate by centrifugation and filtration. We have examined the PPC by GPC and, for the 2.5 h preparation, by MALDI−TOF/MS. Even at 16.5% conversion some of the PPC has a very high molecular weight, ca. 200 000 Da (calibrated against polystyrene). See Supporting Information. In the mass spectrum of the low-MW polymers present at 16.5% conversion, we can identify the end groups as −OH and −H. Specifically, we can observe series in $HO-[(PO)_n\text{-}alt\text{-}(CO_2)_m]-H$, where $m = n - 1$, $n - 2$, to $n - 5$. These are all sodiated ions $HO-[(PO)_n\text{-}alt\text{-}(CO_2)_m]-H{\cdot}Na^+$. See Figure 7.

On the basis of the data obtained from Table 1, we propose that the conversion of PO and CO_2 to PPC is primarily limited by the number of active sites. Some sites must be very active since high MW polymer chains are formed early in the reaction. With time the average molecular weight does not increase significantly. Also after 20 h with less than 16% PO remaining, the mixture is very viscous, and conversion to PPC may be limited by mass transport.

In the absence of CO_2, the zinc glutarate polymerizes PO to PPO at 60 °C in a regioregular manner (HTHTHT) and shows some preference in the polymerization of *rac*-PO for the formation of **ii** triads. See

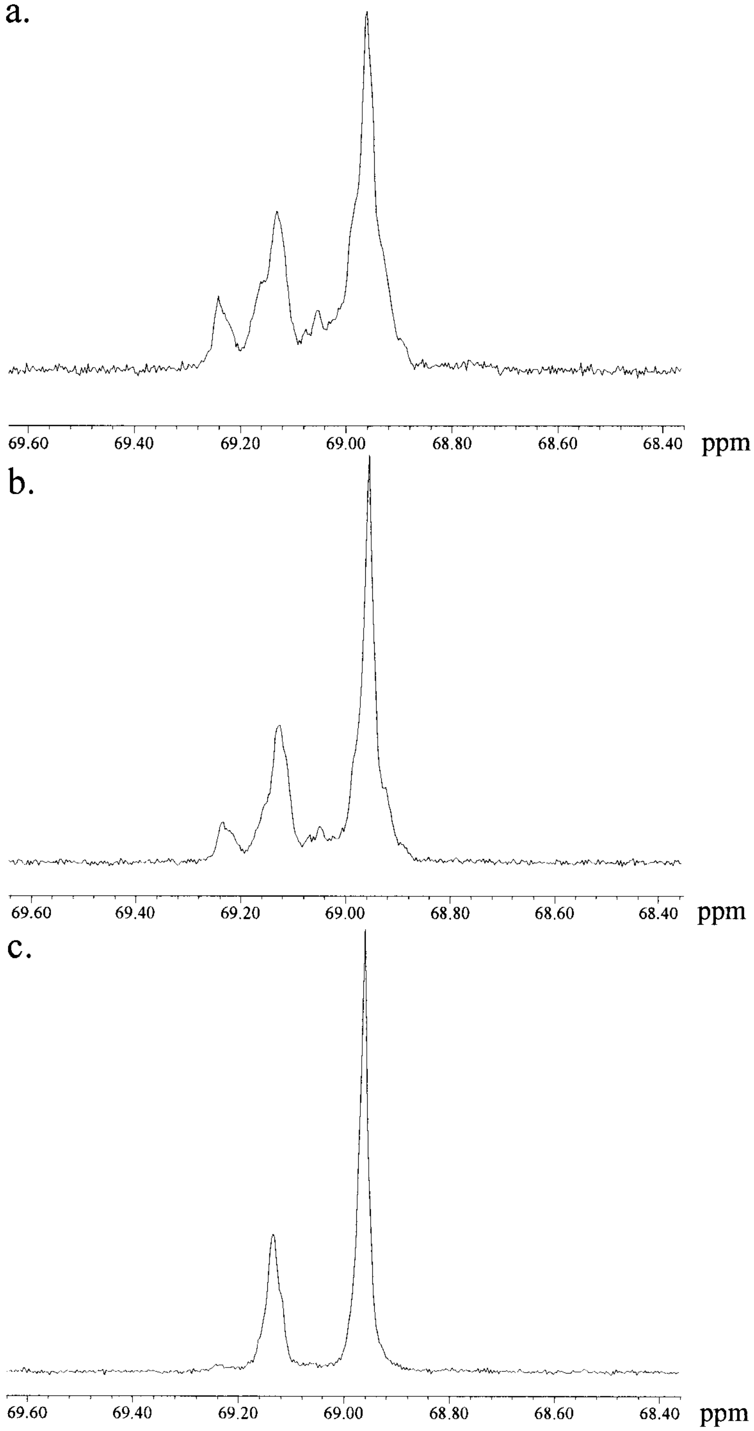

Figure 5. $^{13}C\ \{^{1}H\}$ (150 MHz) NMR spectra of CH_2 region of PPC made from (a) *rac*-PO, (b) 50% *rac*-PO and 50% *S*-PO, and (c) *S*-PO, employing a zinc glutarate catalyst.

Figure 3. By MALDI−TOF/MS we observe that the PPO is −OH and −H terminated, $HO-[(PO)_n]-H\cdot Na^+$, with just a trace amount of cycles $[(PO)_n]\cdot Na^+$. See Figure 8.

3. Degradation of PPC. Since a heterogeneous catalyst may have many different active sites, it is important to determine whether the minor products detected by NMR, such as PC and polyethers, are formed separately or are formed competitively during PPC production. For example, by NMR spectroscopy, it is not easy to distinguish between a small amount of PPO being present or PPC having some deficiency in carbonate such that there are sections in the polymer that have $(PO)_n$ units bounded by carbonates. To investigate the latter, we have degraded the PPC by reaction with LiO^tBu in THF in the presence of ^tBuOH. Within 3 h at room temperature PPC was degraded to PC. The mechanism of the reaction presumably involves alkoxide ion attack on the carbonate carbon followed by backbiting. This effectively unzips the linear polymer producing the cyclic carbonate. A similar result will occur if a hydroxyl end group reacts with LiO^tBu to give ^tBuOH and LiOP. See Scheme 7. A polyether link, however, is not degraded by this mechanism, and PPO is inert to LiO^tBu under the conditions described. The

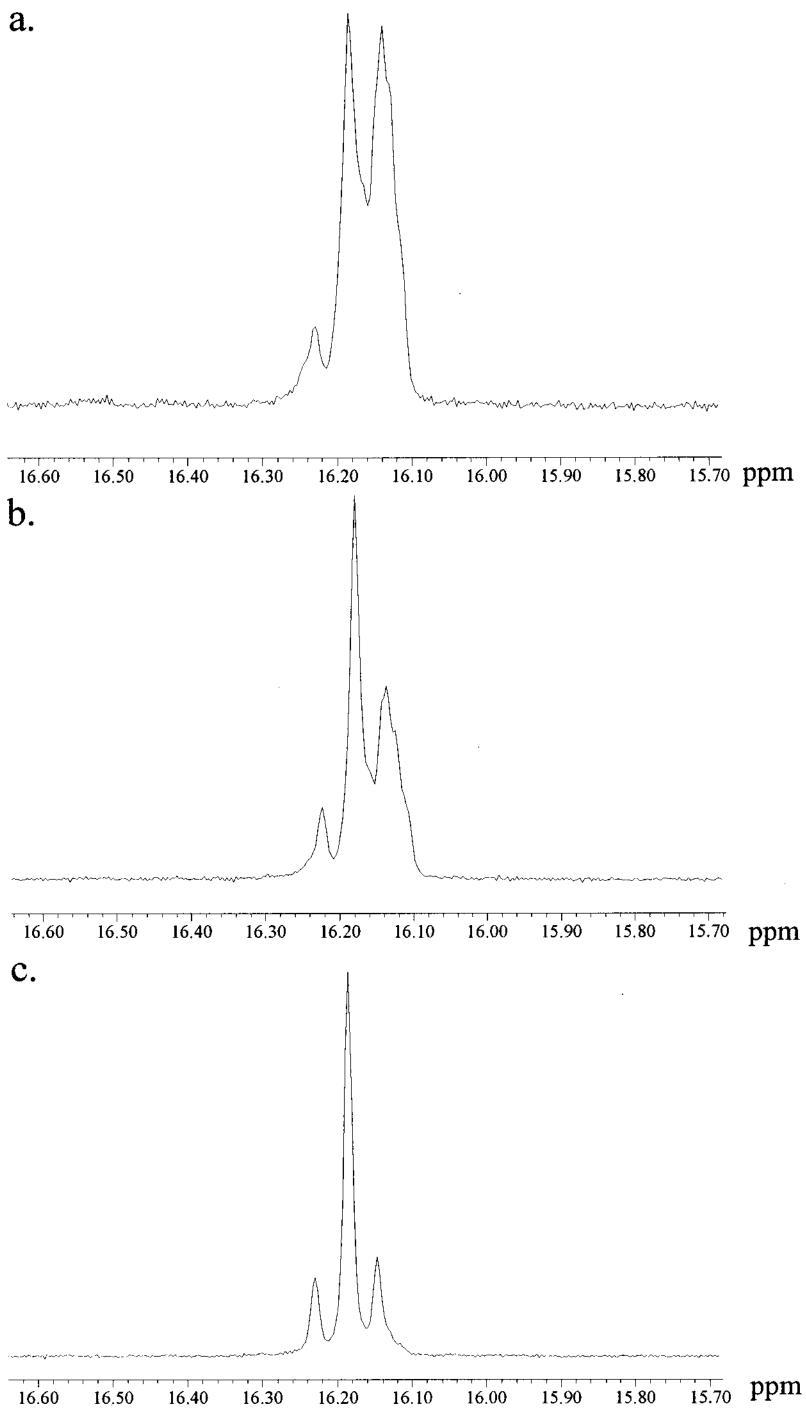

Figure 6. $^{13}C\ \{^{1}H\}$(150 MHz) NMR spectra of CH_3 region of PPC made from (a) *rac*-PO, (b) 50% *rac*-PO and 50% *S*-PO, and (c) *S*-PO, employing a zinc glutarate catalyst.

degraded polymer product has been examined by NMR, GPC, and ESI-QTOF/MS. The major product ca. 98% was PC, and no long chain polyether was detected. However, by mass spectrometry we did detect some small oligomers of the form $HO-[(PO)_n(CO_2)]-H$, $HO-[(PO)_n\text{-}alt\text{-}(CO_2)_2]-H$, and cycles $[(PO)_n(CO_2)]$, where $n = 3, 4, 5, 6$ and trace amounts where $n = 7$ and 8. In addition, we can detect $HO-[(PO)_2]-H\cdot Na^+$ and $[(PO)_3]\cdot H^+$ as ions lacking in CO_2. See Figure 9. This implies that the NMR evidence for polyether formation arises from $(PO)_n$ units ($n \geq 2$) in the PPC chain. This conclusion is also supported by the observed mass spectrum of low-molecular-weight PPC which shows the PO-rich chains (see Figure 6).

Since the work of Kuran[12] previously established that certain organozinc compounds could be catalysts for both the production and degradation of PPC, we questioned whether zinc glutarate could degrade PPC leading with time to the appearance of small quantities of PC. From the mass spectral data, we infer that a hydroxyl group is the initiator, and this Zn−OH group could behave similarly to LiO^{t}Bu. To test this notion, we allowed a commercial sample of PPC of MW ~ 50 000 Da to react with the zinc glutarate catalyst in CH_2Cl_2 at 60 °C for 40 h. After this time we examined the products by GPC and NMR spectroscopy. Some PC was found to have been formed ca. 2% based on PPC. More significantly, however, the molecular weight of the

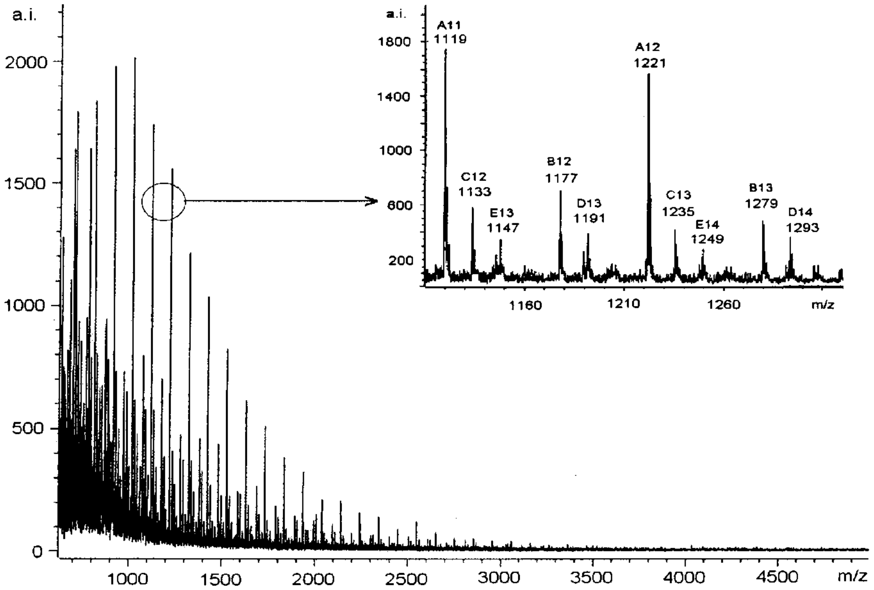

Figure 7. MALDI−TOF mass spectrum of PPC prepared with a zinc glutarate catalyst ($t = 2.5$ h). An = HO−[(C_3H_6O)$_n$-*alt*-(CO_2)$_{n-1}$]−H·Na$^+$, $n = 11, 12$; Bn = HO−[(C_3H_6O)$_n$-*alt*-(CO_2)$_{n-2}$]−H·Na$^+$, $n = 12, 13$; Cn = HO−[(C_3H_6O)$_n$-*alt*-(CO_2)$_{n-3}$]−H·Na$^+$, $n = 12, 13$; Dn = HO−[(C_3H_6O)$_n$-*alt*-(CO_2)$_{n-4}$]−H·Na$^+$, $n = 13, 14$; En = HO−[(C_3H_6O)$_n$-*alt*-(CO_2)$_{n-5}$]−H·Na$^+$, $n = 13, 14$.

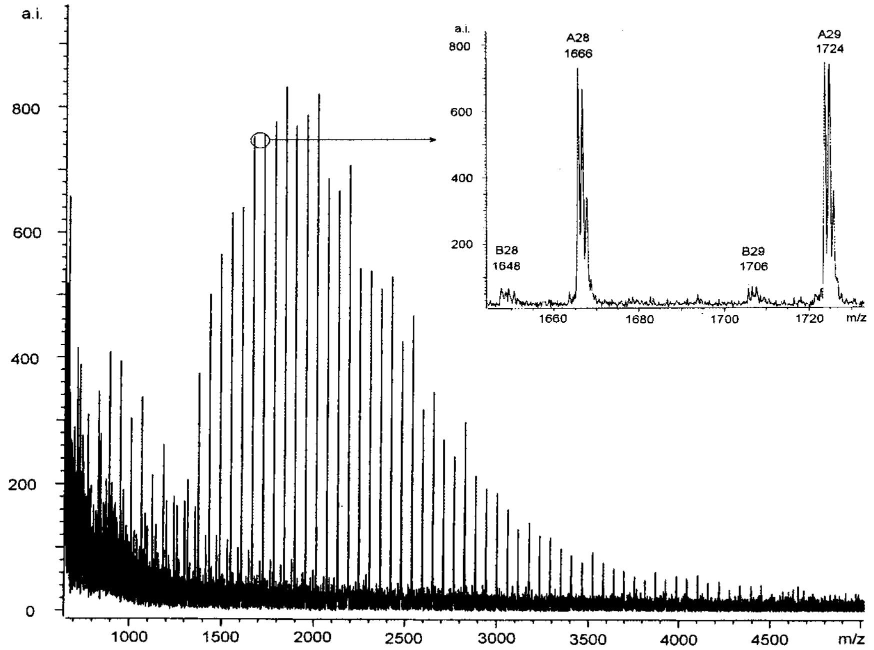

Figure 8. MALDI−TOF mass spectrum of PPO prepared with zinc glutarate. An = HO−[(C_3H_6O)$_n$]−H·Na$^+$, $n = 28, 29$; Bn = [(C_3H_6O)$_n$]·Na$^+$, $n = 28, 29$.

polymer was decreased, and there was evidence of smaller chains with MW ∼ 4000 Da (polystyrene equivalent). However, after 1 week under similar conditions the PPC polymer showed little degradation. We can conclude that the surface active sites responsible for the production of PPC from PO and CO_2 are not very active in PPC degradation, although we have found some evidence of PC formation and chain breaking.

Concluding Remarks

The zinc glutarate catalyst system is active in the polymerization of PO and in the copolymerization of PO and CO_2 by active Zn−OH groups. The surface Zn−OH groups that are active in the conversion of PO to PPO in the absence of CO_2 are active in the production of PPC in the presence of CO_2 (50 bar). Hydroxyl groups have been identified as the end groups by mass spectrometry. The polymerization of PO gives regioregular PPO which is enhanced in isotactic triads. In the formation of PPC we have found preference for the regioregular HT carbonate junctions, but the polymer contains roughly 30% regioirregular HH and TT junctions. By use of ^{13}C {^1H} NMR spectroscopy, we can observe tetrad and triad sensitivity for the carbonate and propylene carbon atoms, respectively, and by use of *S*-PO certain stereosequences have been assigned.

The zinc glutarate catalyst has been found to contain some very active sites for PPC formation as judged by the formation of high molecular weight PPC at short

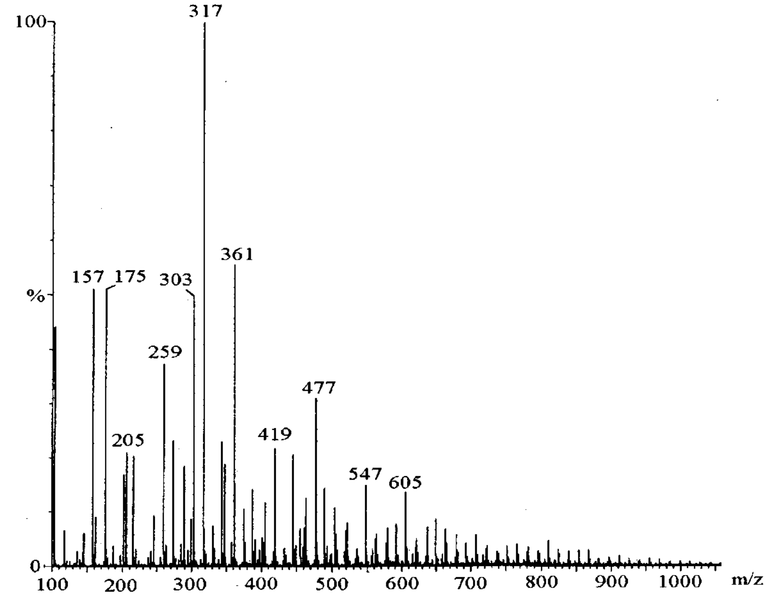

Figure 9. ESI-QTOF mass spectrum of PPC degradation products by LiO^{t}Bu. Peak at m/z = 157 for HO−[(PO)$_2$]−H·Na$^+$, m/z = 175 for [(PO)$_2$]·H$^+$, m/z = 205 for [(PO)$_2$-*alt*-(CO$_2$)$_2$]·H$^+$, m/z = 259 for HO−[(PO)$_3$(CO$_2$)$_1$]−H·Na$^+$, m/z = 303 for HO−[(PO)$_3$-*alt*-(CO$_2$)$_2$]−H·Na$^+$, m/z = 317 for HO−[(PO)$_4$(CO$_2$)$_1$]−H·Na$^+$, m/z = 361 for HO−[(PO)$_4$-*alt*-(CO$_2$)$_2$]−H·Na$^+$, m/z = 419 for HO−[(PO)$_5$-*alt*-(CO$_2$)$_2$]−H·Na$^+$, m/z = 477, HO−[(PO)$_6$-*alt*-(CO$_2$)$_2$]−H·Na$^+$, m/z = 547 for [(PO)$_6$-*alt*-(CO$_2$)$_4$]·Na$^+$, m/z = 605 for [(PO)$_7$-*alt*-(CO$_2$)$_4$]·Na$^+$.

Scheme 5. Eight Possible Regiosequences for Methylene Carbons (*) in PPC at the Triad Level: (4, 5), (3, 6), (2, 7), and (1, 8) Are Four Distinguishable Sequences by NMR Spectroscopy[a]

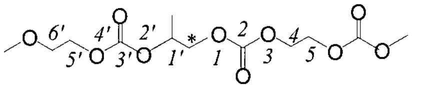

(H.T)	(HT)(H.T)(HT)	*(6', 1', 4)*	1
	(TH)(H.T)(HT)	*(5', 1', 4)*	2
	(HT)(H.T)(TH)	*(6', 1', 5)*	3
	(TH)(H.T)(TH)	*(5', 1', 5)*	4

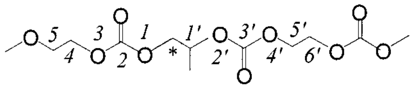

(T.H)	(HT)(T.H)(HT)	*(5, 1', 5')*	5 = 4
	(HT)(T.H)(TH)	*(5, 1', 6')*	6 = 3
	(TH)(T.H)(HT)	*(4, 1', 5')*	7 = 2
	(TH)(T.H)(TH)	*(4, 1', 6')*	8 = 1

[a] The numbers in the brackets indicate the positions of the neighboring methine groups for that regiosequence.

reaction times and low percent conversion. The catalyst is relatively inert to the degradation of PPC. The challenge thus remains to design a molecular system that mimics the active site and does not endear itself to backbitting and PC formation, which appears to be the common mode of reaction of single-site metal alkoxide catalysts. Reactions employing zinc aggregates with active hydoxyl groups will be explored in future studies.

Scheme 6. Eight Possible Regiosequences for Methyl Carbons (*) in PPC at the Triad Level: (4, 5), (2, 6), (3, 7), and (1, 8) Are Four Distinguishable Sequences by NMR Spectroscopy[a]

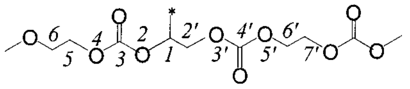

(H.T)	(HT)(H.T)(HT)	*(6, 6')*	1	0.75 x 0.75 x 0.75 = 0.422
	(HT)(H.T)(TH)	*(6, 7')*	2	0.75 x 0.75 x 0.25 = 0.141
	(TH)(H.T)(HT)	*(5, 6')*	3	0.25 x 0.75 x 0.75 = 0.141
	(TH)(H.T)(TH)	*(5, 7')*	4	0.25 x 0.75 x 0.25 = 0.047

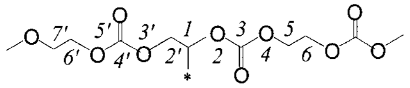

(T.H)	(HT)(T.H)(HT)	*(7', 5)*	5 = 4	0.75 x 0.25 x 0.75 = 0.141
	(HT)(T.H)(TH)	*(7', 6)*	6 = 2	0.75 x 0.25 x 0.25 = 0.047
	(TH)(T.H)(HT)	*(6', 5)*	7 = 3	0.25 x 0.25 x 0.75 = 0.047
	(TH)(T.H)(TH)	*(6', 6)*	8 = 1	0.25 x 0.25 x 0.25 = 0.016

[a] The numbers in the brackets indicate the positions of the neighboring methine groups for that regiosequence.

Experimental Section

All syntheses and solvent manipulations were carried out under an inert atmosphere using standard Schlenk-line and drybox techniques. Solvents were distilled from sodium benzophenone ketyl. Propylene oxide (Fisher) was distilled from calcium hydride. Zinc glutarate was synthesized according to the literature[6] from zinc oxide (Fisher) and glutaric acid (Fisher). CO$_2$ (99.99%) was obtained from BOC Gases. Deuterated solvents were stored over 4 Å molecular sieves for 24 h prior to use.

NMR Experiments. ^{1}H and ^{13}C {^{1}H} NMR experiments were carried out with a Bruker DPX-400 spectrometer equipped

Scheme 7. Two Possible Mechanisms of PPC Degradation by LiO^{t}Bu

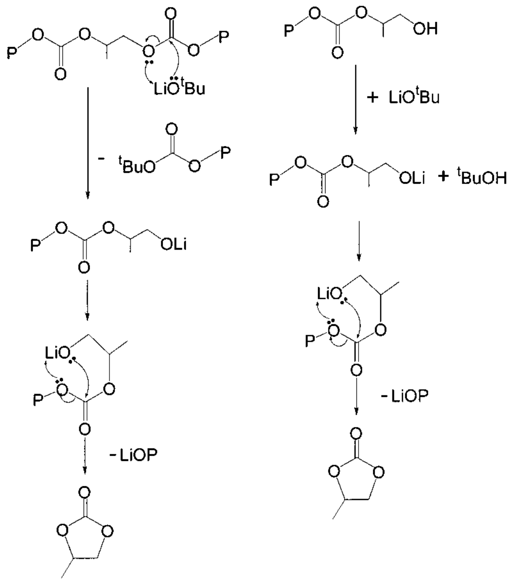

with a 5 mm broad-band probe, a Bruker DPX-500 (5 mm broad-band probe), a Bruker DXR-600 (5 mm broad-band probe), and a Bruker DXR-800 (5 mm TXI probe) spectrometer, operating at proton Larmor frequencies of 400, 500, 600, and 800 MHz, respectively. The parameters used in Bruker DXR-600 and Bruker DXR-800 spectrometers were as follows: number of scans, NS = 2048, number of data point, TD = 65 536, sweep width, swh = 30 303 Hz (600 MHz), swh = 40 322 Hz (800 MHz), and relaxation time, D1 = 1 s. Their peak frequencies were referenced against the solvent, chloroform-*d*, at 7.24 ppm. The deconvolution of ^{13}C NMR spectra was done using Xwin-NMR version 2.6 software.

Mass Spectrometries. The polymer samples obtained in short time polymerization reactions were analyzed by matrix-assisted laser desorption/ionization time-of-flight mass spectroscopy (MALDI−TOF/MS). MALDI−TOF was performed on a Bruker Reflex III (Bruker, Breman, Germany) mass spectrometer operated in linear, positive ion mode with a N_2 laser. Laser power was used at the threshold level required to generate signal. The accelerating voltage was set to 28 kV. The instrument was calibrated with protein standards bracketing the molecular weights of the samples. Matrix 2,5-dihydroxybenzoic acid (DHBA) was prepared as saturated solutions in THF. Allotments of 10 mL of matrix and 2 mL of sample were thoroughly mixed together; 0.5 mL of this was spotted on the target plate and allowed to dry.

The degraded products of PPC were characterized by electrospray ionization mass spectrometry (ESI/MS). The experiment was performed on a Micromass Q-Tof(tm) II (Micromass, Wythenshawe, UK) mass spectrometer equipped with an orthogonal electrospray source (Z-spray) operated in positive ion mode. Sodium iodide was used for mass calibration for a calibration range of m/z 100−2000. The sample was prepared in a solution containing THF infused into the electrospray source at a rate of 5−10 mL min^{-1}. Optimal ESI conditions were capillary voltage 3000 V, source temperature 110 °C, and a cone voltage of 60 V. The ESI gas was nitrogen. Q1 was set to optimally pass ions from m/z 100−2000, and all ions transmitted into the pusher region of the TOF analyzer were scanned over m/z 100−1000 with a 1 s integration time. Data were acquired in the continuum mode until acceptable averaged data were obtained.

GPC Measurements. Gel permeation chromatographic analysis was performed at 35 °C on a Waters Breeze system equipped with a Waters 410 refractive index detector and a set of three columns, Waters Styragel HR-2, HR-4, and HR-6 (Milford, MA). THF (HPLC grade) was used as the eluent at 1.0 mL/min. The sample concentration was 0.1%, and the injection volume was 100 μL. The catalyst residue was removed from the solution by centrifugation and filtration. The calibration curve was made with nine polystyrene standards covering the molecular weight range from 580 to 3 150 000 Da.

DSC Measurements. The DSC experiments were performed on a Perkin-Elmer Pyris 1 differential scanning calorimeter with a Perkin-Elmer Intracooler 1P cooling accessory (Norwalk, CT). The measurements were made in aluminum crimped pans with a heating rate of 10 °C/min, under nitrogen at a flow rate of 20 mL/min.

Copolymerization of PO and CO_2 as a Function of Time. A number of neat PO/CO_2 reactions were carried out at 60 °C in the autoclave, with PO (2 mL, 29 mmol), CO_2 (50 bar), and zinc glutarate (0.1 g, 0.5 mmol), for 2.5, 5, 10, 20, and 40 h. The components in the autoclave right after the reactions were analyzed by ^{1}H NMR spectroscopy. The data are summarized in Table 1.

PPC obtained in the 2.5 h reaction was also analyzed by MALDI−TOF/MS and GPC. MALDI/MS data: All peaks reported correspond to $HO-[(C_3H_6O)_n\text{-}alt\text{-}(CO_2)_m]-H\cdot Na^+$ ions, $m = n - 1$, $n - 2$, $n - 3$, $n - 4$, and $n - 5$, peaks at m/z = 1120 for $n = 11$, $m = 10$, m/z = 1134 for $n = 12$, $m = 9$, m/z = 1148 for $n = 13$, $m = 8$, m/z = 1178 for $n = 12$, $m = 10$, m/z = 1192 for $n = 13$, $m = 9$, m/z = 1222 for $n = 12$, $m = 11$, m/z = 1236 for $n = 13$, $m = 10$, m/z = 1250 for $n = 14$, $m = 9$, m/z = 1280 for $n = 13$, $m = 11$, m/z = 1294 for $n = 14$, $m = 10$. GPC data: M_n = 26 580, M_w = 241 953, MP = 188 079, and PDI = 9.1.

Copolymerization Reactions for PPC Microstructural Studies. Typical copolymerization reactions of PO and CO_2 were done in an autoclave. 0.1 g (0.5 mmol) of zinc glutarate was added into 2 mL (29 mmol) of PO. CO_2 was then added to this system. The system was sealed and heated at 60 °C for 20 h, under a CO_2 pressure of 50 bar. The product was dissolved in benzene and precipitated in methanol. The final products were analyzed by NMR, GPC, and DSC.

rac-PO/CO_2/Zinc Glutarate. ^{1}H NMR ($CDCl_3$, δ, ppm): 1.29, 1.31 (d, CH_3 of PPC), 4.05−4.23 (m, CH_2), 4.90−5.02 (m, CH). DEPT NMR ($CDCl_3$, δ, ppm): CH_3 carbons: 16.61, 16.64, 16.69. CH_2 carbons: 69.42, 69.52, 69.60, 69.69. CH carbons: 72.52, 72.57, 72.76, 72.80. ^{13}C {^{1}H} NMR (50 mg/mL, $CDCl_3$, δ, ppm): 16.14, 16.19, 16.23 (m, CH_3 of PPC), 68.96, 69.05, 69.08, 69.14, 69.24 (m, CH_2), 72.03, 72.08, 72.32, 72.33, 72.34 (m, CH), 153.65, 153.67, 153.70, 153.78, 153.80, 153.83 (m, C═O, H−H region), 154.14, 154.17, 154.19, 154.21, 154.23, 154.25, 154.27 (m, C═O, H−T), 154.64, 154.66 (m, C═O, T−T). GPC data: M_n = 66 326, M_w = 458 616, MP = 415 747, and PDI = 6.9. DSC data: glass transition temperature T_g = 26.8 °C, decomposition temperature T_d = 264.7 °C.

S−PO/CO_2/Zinc Glutarate. ^{1}H NMR ($CDCl_3$, δ, ppm): 1.32, 1.34 (d, CH_3 of PPC), 4.12−4.30 (m, CH_2), 4.94−5.05 (m, CH). DEPT NMR ($CDCl_3$, δ, ppm): CH_3 carbons: 16.22, 16.25, 16.30. CH_2 carbons: 69.03, 69.20. CH carbons: 72.14, 72.18, 72.38, 72.41. ^{13}C {^{1}H} NMR (50 mg/mL, $CDCl_3$, δ, ppm): 16.15, 16.19, 16.23 (m, CH_3 of PPC), 68.97, 69.14 (m, CH_2), 72.07, 72.08, 72.11, 72.31, 72.34 (m, CH), 153.63, 153.64, 153.67 (m, C═O, H−H region), 154.14, 154.16 (m, C═O, H−T), 154.63, 154.64 (m, C═O, T−T). GPC data: M_n = 17 479, M_w = 243 017, MP = 28 201, and PDI = 13.9. DSC data: T_g = 37.8 °C and T_d = 219.4.

50% rac-PO/50% S−PO/CO_2/Zinc Glutarate. ^{13}C {^{1}H} NMR (50 mg/mL, $CDCl_3$, δ, ppm): 16.14, 16.18, 16.22 (m, CH_3 of PPC), 68.93, 68.96, 69.05, 69.07, 69.13, 69.23 (m, CH_2), 72.00, 72.03, 72.06, 72.07, 72.10, 72.31, 72.33 (m, CH), 153.62, 153.64, 153.66, 153.69, 153.77, 153.80, 153.82 (m, C═O, H−H region), 154.14, 154.16, 154.18, 154.20, 154.22, 154.24, 154.26 (m, C═O, H−T), 154.63, 154.65 (m, C═O, T−T). GPC data: M_n = 20 268, M_w = 249 464, MP = 74 610, and PDI = 12.3. DSC data: T_g = 40.7 °C and T_d = 218.1.

Homopolymerization of PO. The catalyst (0.1 g, 0.5 mmol) was allowed to react with *rac*-PO (2 mL, 29 mmol) at 60 °C for 5 h. The residue of the catalyst was removed by dissolving the product in benzene. The excess monomer, benzene, and any other volatiles species were evaporated under vacuum to give a white polymer, yield 72.4%. The polymer was analyzed by ^{1}H NMR, ^{13}C {^{1}H} NMR, GPC, and MALDI−TOF/MS. ^{1}H NMR ($CDCl_3$, δ, ppm): 0.98−1.04 (m, CH_3 of PPO), 3.15−3.65 (m, CH_2 and CH of PPO). ^{13}C {^{1}H} NMR ($CDCl_3$, δ, ppm): 17.28, 17.39 (m, CH_3 of PPO), 72.77, 72.83, 72.87, 72.92, 73.32, 73.35, 73.37 (m, CH_2 of PPO), 75.08, 75.28, 75.32, 75.48 (m, CH of PPO). GPC data: M_n = 12 443, M_w = 485 752, MP = 4394, and PDI = 39.0 (PDI = 7.4 after precipitated in methanol). MALDI/MS data: Two series are found: the major one is $HO-[(C_3H_6O)_n]-H\cdot Na^+$ ions, and the other is $[(C_3H_6O)_n]Na^+$, with no end groups. Peak at m/z = 1648 for $[(C_3H_6O)_{28}]\cdot Na^+$, m/z = 1666 for $HO-[(C_3H_6O)_{28}]-H\cdot Na^+$, m/z = 1706 for $[(C_3H_6O)_{29}]Na^+$, and m/z = 1724 for $HO-[(C_3H_6O)_{29}]-H\cdot Na^+$.

Degradation Studies of PPC. Degradation reaction of 0.5 g of PPC was done in THF at room temperature for 3 h, under an inert atmosphere, using 10 mg (0.12 mmol) of LiO^{t}Bu (Aldrich) and 0.02 mL (0.3 mmol) of ^{t}BuOH (Aldrich). The product was analyzed by ^{1}H NMR, GPC, and ESI/MS. ^{1}H NMR ($CDCl_3$, δ, ppm): 1.39, 1.40 (d, CH_3 of PC), 3.10−3.70 (m, trace, CH_2 and CH of PPO), 3.93, 3.95, 3.97, 4.46, 4.48, 4.50 (m, CH_2 of PC), 4.74, 4.76, 4.78, 4.80, 4.81, 4.83 (m, CH of PC). GPC data: M_n = 542, M_w = 630, MP = 494, and PDI = 1.16. ESI/MS data: peak at m/z = 157 for $HO-[(PO)_2]-H\cdot Na^+$, m/z = 175 for $[(PO)_2]\cdot H^+$, m/z = 205 for $[(PO)_2\text{-}alt\text{-}(CO_2)_2]\cdot H^+$, m/z = 259 for $HO-[(PO)_3(CO_2)_1]-H\cdot Na^+$, m/z = 303 for $HO-[(PO)_3\text{-}alt\text{-}(CO_2)_2]-H\cdot Na^+$, m/z = 317 for $HO-[(PO)_4(CO_2)_1]-H\cdot Na^+$, m/z = 361 for $HO-[(PO)_4\text{-}alt\text{-}(CO_2)_2]-H\cdot Na^+$, m/z = 419 for $HO-[(PO)_5\text{-}alt\text{-}(CO_2)_2]-H\cdot Na^+$, m/z = 477, $HO-[(PO)_6\text{-}alt\text{-}(CO_2)_2]-H\cdot Na^+$, m/z = 547 for $[(PO)_6\text{-}alt\text{-}CO_2)_4]\cdot Na^+$, and m/z = 605 for $[(PO)_7\text{-}alt\text{-}(CO_2)_4]\cdot Na^+$.

0.75 g of PPC obtained from Aldrich was allowed to react with 50 mg (0.26 mmol) of zinc glutarate in 10 mL of CH_2Cl_2 at 60 °C for 40 h under an inert atomosphere. The product was analyzed by ^{1}H NMR and GPC. The ratio of PC/PPC increased from 2.51% to 4.39%. See Supporting Information.

Acknowledgment. We thank the Department of Energy, Office of Basic Sciences, Chemistry Division, for financial support of this work. The mass spectrometers were purchased by a grant from the Hayes Investment Fund of the Ohio Board of Regents. We also thank the staff of the Campus Chemical Instrument Center (CCIC) for running the samples in NMR and Mass spectrometers.

Supporting Information Available: Deconvolution data for the ^{13}C {^{1}H} NMR spectra from the polymers obtained from *rac*-PO and CO_2, *S*-PO and CO_2, 50% *rac*-PO + 50% *S*-PO, and CO_2 with zinc glutarate, as well as statistical calculations for the probability of ring-opening at the methine or methylene carbon during PPC formation, statistical calculations for the different regiosequences of carbonate carbons at the tetrad level, statistical calculations for the stereosequences of the (HT)(HT).(HT)(HT) regiosequence of cabonate carbons in PPC made from 50% *rac*-PO + 50% *S*-PO, and statistical calculations for the regiosequences of methine, methylene, and methyl carbons in PPC at the triad level; GPC traces of PPCs obtained in 2.5, 5, 10, 20, and 40 h reactions, ^{1}H NMR spectrum and GPC data for the degradation product of PPC by LiO^{t}Bu, and GPC of the product of the reaction between commercial PPC and zinc glutarate for 40 h. This material is available free of charge via the Internet at http://pubs.acs.org.

References and Notes

(1) (a) Inoue, S.; Koinuma, H.; Tsuruta, T. *J. Polym. Sci., Polym. Lett.* **1969**, *7*, 287−292 (b) Inoue, S.; Koinuma, H.; Tsuruta, T. *Makromol. Chem.* **1969**, *130*, 210−220.

(2) (a) Rokicki, A.; Kuran, W. *J. Macromol. Sci., Rev. Macromol. Chem.* **1982**, *C* (21), 135−186. (b) Darensbourg, D.; Holtcamp, M. *Coord. Chem. Rev.* **1996**, *153*, 155−174. (c) Super, M. S.; Beckman, E. J. *TRIP* **1997**, *5*, 236−240.

(3) Ree, M.; Bae, J. Y.; Jung, J. H.; Shin, T. J. *Korea Polym. J.* **1999**, *7*, 333−349.

(4) Kuran, W.; Pasynkiewicz, S.; Skupinska, J.; Rokicki, A. *Makromol. Chem.* **1976**, *177*, 11−20.

(5) (a) Aida, T.; Inoue, S. *J. Am. Chem. Soc.* **1985**, *107*, 1358−1364. (b) Aida, T.; Ishikawa, M.; Inoue, S. *Macromolecules* **1986**, *19*, 8−13.

(6) Ree, M.; Bae, J. Y.; Jung, J. H.; Shin, T. J. *J. Polym. Sci., Part A: Polym. Chem.* **1999**, *37*, 1863−1876.

(7) Chamberlain, B. M.; Cheng, M.; Moore, D. R.; Ovitt, T. M.; Lobkovsky, E. B.; Coates, G. W. *J. Am. Chem. Soc.* **2001**, *123*, 3229−3238.

(8) Chisholm, M. H.; Gallucci, J.; Phomphrai, K., unpublished results.

(9) Behr, A. *Carbon Dioxide Activation by Metal Complexes*; VCH Publishers: New York, 1988; pp 91−93.

(10) Lednor, P. W.; Rol, N. C. *J. Chem. Soc., Chem. Commun.* **1985**, *9*, 598−599.

(11) (a) Shimasaki, K.; Aida, T.; Inoue, S. *Macromolecules* **1987**, *20*, 3076−3080. (b) Aida, T.; Inoue, S. *J. Am. Chem. Soc.* **1983**, *105*, 1309−1316.

(12) (a) Kuran, W.; Gorecki, P. *Makromol. Chem.* **1983**, *184*, 907−912. (b) Gorecki, P.; Kuran, W. *J. Polym. Sci., Polym. Lett.* **1985**, *23*, 299−304.

MA020348+